

# Relaxation kinetics in two-dimensional structures

José L. Iguain and Laurent J. Lewis

*Département de Physique et Groupe de Recherche en Physique et Technologie des Couches Minces (GCM)  
Université de Montréal, Case Postale 6128, Succursale Centre-Ville, Montréal, Québec H3C 3J7, Canada.*

(Dated: May 1, 2019)

We have studied the approach to equilibrium of islands and pores in two dimensions. The two-regime scenario observed when islands evolve according to a set of particular rules, namely relaxation by steps at low temperature and smooth at high temperature, is generalized to a wide class of kinetic models and the two kinds of structures. Scaling laws for equilibration times are analytically derived and confirmed by kinetic Monte Carlo simulations.

PACS numbers: 61.46.+w

## I. INTRODUCTION

A large amount of work has been done in the domain of atomic structure kinetics since Burton, Cabrera and Frank presented, in a seminal paper, the first serious attempt to model the behavior of atoms adsorbed onto a vicinal surface<sup>1</sup>. Nevertheless, several problems remain unsolved. Many important advances in the techniques for the observation and manipulation of atoms now allow dealing with structures of decreasing size and, with the help of powerful computation, gaining insight into the basic mechanisms governing atomic dynamics. (For a review, see for example Ref. 2,3,4 and references therein).

In the last few years, considerable efforts have been dedicated to understanding how nanostructures relax. A classical description of structure shape equilibration was developed by Herring, Nichols and Mullins (HNM)<sup>5</sup>. In this theory, the transport of mass responsible for relaxation occurs in a smooth and continuous way via migration of border adatoms from regions of high curvature (high chemical potential  $\mu$ ) to regions of low curvature (low  $\mu$ ). It is assumed that structure border is rough enough to allow a continuous (coarse-grained) description of it. However, as this is not valid for surfaces below the roughening temperature, the low temperature decay has been the subject of research both theoretically<sup>6,7,8</sup> and experimentally<sup>9,10</sup>.

Recently, studies of two-dimensional island shape relaxation with a simple model has revealed new, unexpected phenomena<sup>6,7</sup>. It was shown that two qualitatively different relaxation regimes exist. At high temperature, islands evolve toward equilibrium according to HNM. At low temperature, islands become faceted and a new driving mechanism appears. It was demonstrated that, in this case, shape relaxation occurs by steps, where the limiting process consists in the nucleation of new adatom rows on the flat edges of islands. In the above model adatoms lie on a triangular lattice and both equilibrium and kinetic properties depend on the single parameter  $\epsilon_0/k_B T$  (where  $k_B$  is the Boltzmann constant and  $T$  the temperature) since, for an adatom with  $n_i$  nearest-neighbors (NN),  $n_i \epsilon_0$  is both the potential energy and the kinetic barrier controlling migration.

This two-regime scenario is manifest in the depen-

dence of the equilibration time  $t_{eq}$  on temperature and island size  $N$ . At high temperature,  $t_{eq} \sim N^2 \exp(3\beta\epsilon_0)$  ( $\beta = 1/k_B T$ ), while at low  $T$ ,  $t_{eq} \sim N \exp(4\beta\epsilon_0)$ . The regime to which relaxation of a given island belongs is determined by border roughness and depends not only on temperature but also on island size. In the  $T-N$  plane, the separation line between the two regimes is provided by the crossover island size  $N_c(T) \sim \exp(\beta\epsilon_0)$ , a rough indication of the size of the largest island that is fully faceted at  $T$ . Interestingly, if the temperature-dependent factors appearing in the leading terms of  $t_{eq}$  are rewritten in terms of  $N_c$ , the properly-scaled equilibration time becomes a function of  $N/N_c$  only, satisfying

$$\left(\frac{t_{eq}}{N_c^5}\right) \sim \begin{cases} \left(\frac{N}{N_c}\right) & \text{for } \frac{N}{N_c} \ll 1 \\ \left(\frac{N}{N_c}\right)^2 & \text{for } \frac{N}{N_c} \gg 1 \end{cases} . \quad (1)$$

A first problem of interest is the universality of this scaling law. The model described above is at best a first approximation to real situations and many details can be modified in order to improve it. For example, such a well-known effect as the Ehrlich-Schwoebel barrier<sup>11</sup> can be accounted for by introducing new kinetic barriers in a phenomenological way; in an even more accurate approach, minimum energy transition paths could be calculated from interatomic forces<sup>12</sup>. As a different set of kinetic barriers will entail, to the least, new activation energies, the question remains whether the above scaling behavior is a consequence of the model or, to the contrary, would carry over to more general situations.

Another closely-related problem is the relaxation of two-dimensional *pores*, i. e., islands of *vacancies*. In some sense, islands and pores are ‘specular images’ of one another. A given pore has the same boundary as the corresponding island, and so would be faceted or rough depending on whether the number of *vacancies* in it is smaller or larger than  $N_c(T)$ . It would be desirable to know if pore shape relaxation exhibits also a two-regime scenario and to analyze the possibility of scaling laws for the corresponding equilibration times.

As far as we know, the questions above have not been

investigated, even in the case of simple models. In this work we study the main properties of shape relaxation in two-dimensional structures of adatoms. Our approach is two-fold: theoretical analysis and numerical simulations. In the analytic part, we treat the shape relaxation problem in a general way. Our study suggests the presence of two regimes, regardless of the specific set of kinetic barriers and, based on detailed-balance conditions, we show that similar scaling laws apply for both islands and pores. Since most of the arguments we invoke are heuristic, some independent confirmation of the derived properties is desirable. This is the goal of the numerical part. We analyze, using standard kinetic Monte Carlo (KMC) simulations, the relaxation of islands and pores according to two models considered in this paper, and compare the results with our theoretical predictions.

The paper is organized as follows. In Sec. II we discuss the causes for scaling behavior and derive the asymptotic laws of scaling functions. The models we use are defined in Sec. III and the outcome of the KMC simulations are presented in Sec. IV. Finally, we give our conclusions in Sec. V.

## II. ANALYTIC APPROACH

In this section we investigate a generic model with adatoms lying on a triangular lattice where the total binding energy per NN pair is  $\epsilon_0$ . Equilibrium properties depend on a single parameter, namely  $\beta\epsilon_0$ , but kinetics involve in general a greater number of them. Our aim here is to establish scaling laws for both island and pore relaxation times.

Let us consider islands first. It is easy to see that many of the arguments presented in Ref. 6,7 remain applicable regardless of the specific set of kinetic barriers. First of all,  $N_c(T)$ , which separates rough and faceted islands at a given temperature, is the size at which the perimeter equals the average distance between border kinks. This does not depend on the transition barriers but only on the binding energies in the different configurations, so the form  $N_c \sim \exp(\beta\epsilon_0)$  is still valid. Next, two qualitatively different modes of relaxation should exist. On the one hand, for islands greater than  $N_c$ , shape relaxation dynamics is adequately described by the HNM theory. It consists of a set of equations for the temporal evolution of the border curvature, where the kinetics is dominated by perimeter diffusion and always leads to a  $t_{eq} \sim N^2$  power law. We will call this regime *rough relaxation mode* (RRM). On the other hand, mechanisms driving islands smaller than  $N_c$  toward equilibrium are also quite general. In this scenario, islands spend most of the time in highly-faceted configurations. We will call this regime *faceted relaxation mode* (FRM). Evolution occurs by steps consisting in nucleation and stabilization of new adatom rows. The time associated to each of these steps is proportional to facet length ( $\sim N^{1/2}$ ) and, given an initial configuration, a number  $\sim N^{1/2}$  of rows needs

to be created in order to attain the equilibrium shape; thus  $t_{eq} \sim N$ .

The size exponents for equilibration time thus appear to be universal (1 in the FRM, 2 in the RRM). The activation energies however *do* depend in general on the kinetic barriers. The activation energy in the FRM corresponds to the energy characteristic of row nucleation, while in the RRM it will be equivalent to the characteristic energy for diffusion along the island border. If we call these energies  $E_F$  and  $E_R$  for the FRM and RRM, respectively, the arguments presented so far allow us to write the ansatz

$$t_{eq} \sim \begin{cases} \left(\frac{N}{N_c}\right) e^{\beta(E_F + \epsilon_0)} & \text{for } \frac{N}{N_c} \ll 1 \\ \left(\frac{N}{N_c}\right)^2 e^{\beta(E_R + 2\epsilon_0)} & \text{for } \frac{N}{N_c} \gg 1 \end{cases} . \quad (2)$$

At this point, it is clear that the occurrence of scaling is limited to the cases where

$$E_F = E_R + \epsilon_0 \quad ; \quad (3)$$

otherwise, the exponential factors in Eq. (2) would be different and no *natural* time scale [such as  $\sim N^5$  in Eq. (1)], allowing scaled  $t_{eq}$  to be expressed as a function of  $N/N_c$ , would exist. Let us, then, analyze the connexion between the two energies.

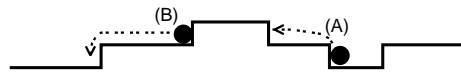


FIG. 1: Schematic of the limiting processes for diffusion along a rough border. Adatom detaches from a kink and go into adjacent rows after jumping around a corner. All the sites below the full line, which represents the border, are occupied.

As noted above, the limiting step in the RRM is adatom border diffusion. This is in turn limited by the elementary processes sketched in Fig. 1, in which adatoms pass from one kink to another by jumping around a corner; thus we can readily equal  $E_R$  and the energy of this process.

For the FRM, the dynamics is determined by row nucleation, which occurs when two adatoms meet on a flat island edge. The nucleation rate may thus be calculated by the product of two factors: the rate of adatoms entering a facet and the probability that another adatom lies on the same facet. In this regime, the main sources of adatoms are facet ends, where the most weakly bound adatoms are found. Those adatoms move onto flat facets by basically the process sketched in Fig. 1 (A); the

first factor is thus  $\sim \exp(-\beta E_R)$ . The second factor is  $\sim \exp(-\beta \epsilon_0)$  because the system gains an energy  $\epsilon_0$  when an adatom moves from a kink to a flat edge. Thus, we have  $E_F = E_R + \epsilon_0$ , i. e., Eq. (3), and the scaling form

$$\frac{t_{eq}}{N_c^\alpha} \sim \begin{cases} \left(\frac{N}{N_c}\right) & \text{for } \frac{N}{N_c} \ll 1 \\ \left(\frac{N}{N_c}\right)^2 & \text{for } \frac{N}{N_c} \gg 1 \end{cases}, \quad (4)$$

where the exponent  $\alpha$  is

$$\alpha = 2 + \frac{E_R}{\epsilon_0}. \quad (5)$$

We consider now the case of pores. Since, as mentioned before, a pore will also be rough or faceted depending on whether it is larger or smaller than  $N_c$ , it is worth analyzing each situation separately.

For the relaxation of rough pores, the solution is immediate: the kinetic path is the same as that followed by the corresponding island (via a vacancy-atom exchange mechanism). This pore-island symmetry is clearly evident in the HNM theory (see for example Ref. 6), which involves only border curvature and perimeter atomic diffusion and hence does not depend on the kind of particles enclosed within the border. As a corollary, the equilibration time for pores should also satisfy the asymptotic law established by the second equation in Eq. (2); this will be verified numerically in Sec. IV.

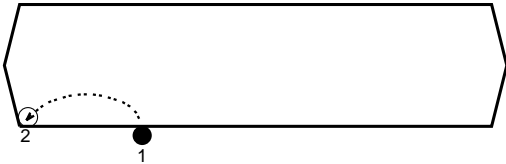


FIG. 2: Schematic of row nucleation in a pore. All adatoms are outside the line which represents the border of a fully faceted pore.

For faceted pores, it is clear that relaxation will occur, as in the case of faceted islands, by steps consisting of the nucleation and stabilization of new rows. However, despite this qualitative analogy, the two processes are not equivalent but, rather, complementary; adatom migration occurs from short to long facets in islands, while the opposite is true in pores. For the latter, row nucleation occurs when, as shown schematically in Fig. 2, an adatom that lies on a long facet moves to an internal corner of the pore. The new row will grow with the arrival of more adatoms from the now ‘open’ long facet, and become stable when fully filled.

The similarity of the relaxation mechanisms allows us to apply, in the case of pores, the same kind of arguments we invoked for the dependence of  $t_{eq}$  on the size of

faceted islands, which again yields the power law  $t_{eq} \sim N$ . In order to calculate the activation energy—which corresponds to the nucleation process illustrated in Fig. 2—we consider first the inverse process, i. e., the migration of an adatom from site **2** to site **1**. In this case, the adatom first leaves a kink, then diffuses along a flat border and, finally, goes into an adjacent row by jumping around a corner. This is similar to the process sketched in Fig. 1 (B) and must therefore have an activation energy  $E_R$ . Knowledge of this last energy allows us to find that corresponding to nucleation. They are related by the detailed-balance condition which, taking into account that the binding energy difference between sites **1** and **2** is  $\epsilon_0$ , finally leads to the result that the activation energies for pore shape relaxation are also connected by relation (3).

As an interesting consequence, the equilibration time for islands or pores, when properly scaled with  $N_c^\alpha$ , becomes a function of  $N/N_c$  only that satisfies the asymptotic rules (4). We stress that even though the HNM theory implies an equivalent relaxation mode for both kinds of structures in the RRM, the same symmetry cannot be expected to hold in the FRM. The asymptotic forms give the exponents of the leading terms but different prefactors may appear. In general, there will be one scaling function corresponding to islands and *another* scaling function for pores. For very small values of their arguments ( $N \ll N_c$ ) they will be parallel (on a log scale) but not necessarily equal, while at the other extreme ( $N \gg N_c$ ) the curves should collapse as required by HNM theory. Using KMC we will see, in Sec. IV, that these properties of the scaling functions are verified.

### III. THE MODELS

In order to assess the analytical predictions above, we investigated two different models, denoted I and II, which have the following common characteristics: The substrate is represented by a triangular lattice and the total binding energy per NN pair is  $\epsilon_0$ . Adatom hoppings are only possible between NN sites and a given adatom in an initial site  $a$  jumps to a final empty site  $b$  with a probability per unit time  $P_{ab} = \nu \exp(-\beta E_{ab})$ , where  $\nu$  is a constant frequency and  $E_{ab}$  the kinetic barrier. In order to avoid detachment, the jumps are forbidden if the number of NN adatoms in the final site is 0. As an additional simplification, the motion of adatoms with initially more than 4 NN is also forbidden. This approximation is justified because of the high energy barriers of the corresponding processes; it is introduced in order to accelerate the simulations. Differences between models I and II lie only in the set of kinetic barriers.

For Model I, which is the same as the one used in Ref. 6,7,  $E_{ab}$  depends only on the number  $n_a$  of NN adatoms in the initial site  $a$ . It takes the value  $E_{ab} = n_a \epsilon_0$  when  $1 < n_a < 5$  and  $E_{ab} = \epsilon_0/10$  when  $n_a = 1$ , regardless of the number of NN adatoms in  $b$ .

For Model II, we use a more accurate set of activation

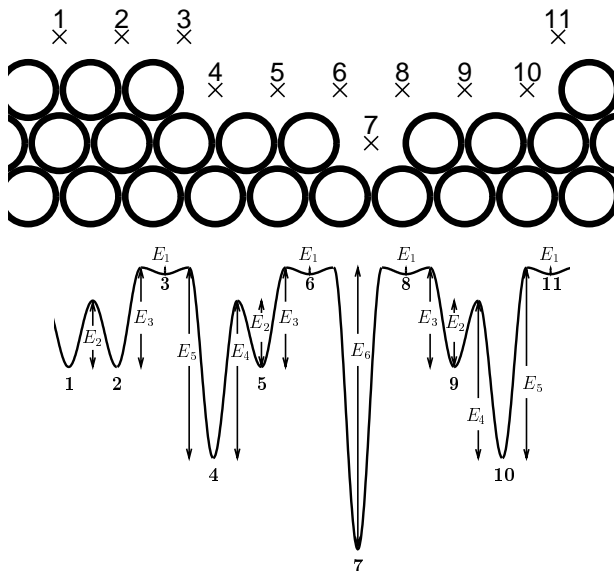


FIG. 3: The energy landscape for Model II.

energies, obtained from a detailed study of the kinetic barriers for adatoms lying on a triangular lattice and interacting via a Lennard-Jones potential<sup>13</sup>. It is useful to define this model with the help of Fig. 3, where the different barriers are represented. In the top part of the figure, adatoms are represented by circles while crosses indicate possible binding sites. The bottom part shows the corresponding energy landscape, i. e., kinetic barriers separating adjacent local minima. Thus, in this model, we take into account the final-state configuration when evaluating the transition-state energy. (Note however that the height of the barrier depends on the number of NN in the initial and final states but not on their precise position). Model II thus incorporates such important features as the Ehrlich-Schwobel barrier. This is apparent if we look at Fig. 3: the barrier from **2** to **1** is lower than the barrier from **2** to **3**; the barrier from **4** to **3** is higher than the barrier from **4** to **5**, etc. The final parameters in this model are  $E_1=0$ ,  $E_2=0.5\epsilon_0$ ,  $E_3=\epsilon_0$ ,  $E_4=1.5\epsilon_0$ ,  $E_5=2\epsilon_0$ ,  $E_6=4\epsilon_0$ . In order to facilitate comparison, Table I lists, for both models, the kinetic barriers corresponding to a given elementary jump as a function of the number of NN before ( $n_i$ ) and after ( $n_f$ ) the hopping.

Before closing this section, we calculate the activation energies for each model as derived from the analysis of Sec. II. Remember that  $E_R$  is the energy characteristic of the process sketched in Fig. 1 (A). For Model I, this process corresponds to an adatom with 3 NN before the jump, so  $E_R^I=3\epsilon_0$ , and, using Eqs. (2) and (5),  $E_F^I=4\epsilon_0$  and  $\alpha^I=5$ , as obtained in Ref. 6,7 (but not yet tested with pores). For Model II, the process in question is (for example) the transition from **4** to **2** in Fig. 3, which leads to  $E_R^{II}=2\epsilon_0$ ,  $E_F^{II}=3\epsilon_0$  and  $\alpha^{II}=4$ .

$n_i$	$\Delta E^I[\epsilon_0]$	$\Delta E^{II}[\epsilon_0]$
1	0.1	0.0
2	2.0	0.5, for $n_f \neq 1$
		1.0, for $n_f = 1$
3	3.0	1.5, for $n_f \neq 1$
		2.0, for $n_f = 1$
4	4.0	4.0

TABLE I: Kinetic barrier for Model I ( $\Delta E^I$ ) and Model II ( $\Delta E^{II}$ ) as a function of the number of NN before ( $n_i$ ) and after ( $n_f$ ) the jump. For Model I, the barriers depend only on  $n_i$ . Detachments, as well as jumps of adatoms with  $n_i > 4$ , are forbidden in both models.

#### IV. NUMERICAL RESULTS

As mentioned in Sec. I, a numerical confirmation of the results of Sec. II, obtained in a heuristic manner, is in order. In this section, we do this using KMC simulations to explore shape relaxation according to models I and II. We consider islands and pores with sizes between 400 and 6500 particles and perform, for each model, standard KMC simulations. The values of  $\beta$  (in  $1/\epsilon_0$  units) range between 2 and 17. The results shown in this section correspond to averages over a number of samples, varying from 4 for the largest structures to 30 for the smallest ones.

Following Ref. 6,7, we use the aspect ratio  $\alpha$ , defined as the ratio of the  $x$  and  $y$  gyration radii, to characterize the state of the structures. We start each simulation with an aspect ratio around 10 and define the equilibration time  $t_{eq}$  as the time at which  $\alpha$  first becomes less than 1. First of all, we analyze the dependence of  $t_{eq}$  on  $N$  (for fixed  $\beta$ ) and, separately, on  $\beta$  (for fixed  $N$ ). Later in this section, we will check the scaling laws.

Let us start with Model I. In order to test the behavior of  $t_{eq}$  as a function of  $N$ , we plot in Fig. 4 (a)  $\ln t_{eq}$  against  $\ln N$  for several temperatures. Filled and empty symbols correspond to islands and pores, respectively. At high (low) enough temperature,  $t_{eq}$  is expected to scale as  $N^2$  ( $N$ ). This scaling behavior is represented in Fig. 4 (a) by the lines with slopes of 2 (lower) and 1 (upper), which bracket the KMC results corresponding to the highest and lowest temperatures used in our simulations, respectively. Using these lines as a guide, it is indeed clear that the size exponent changes from 1 to 2 when the temperature is increased, consistent with the numerical findings. Note that the agreement is as good for pores as it is for islands.

We check now our predictions for the activation energies. To do so, in Fig. 4 (b),  $\ln t_{eq}$  is plotted against  $\beta$  for different sizes. The asymptotic behaviors are represented by the straight lines which have slopes of  $3\epsilon_0$  (low  $\beta$ ) and  $4\epsilon_0$  (high  $\beta$ ). The KMC data again show excel-

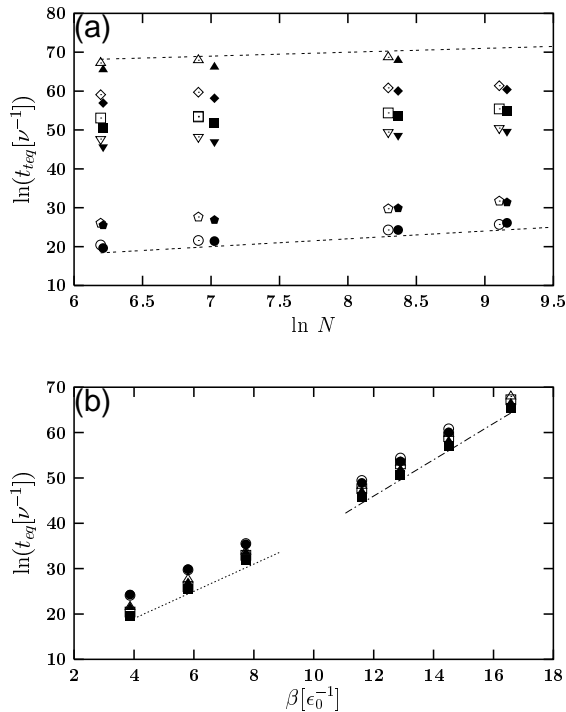


FIG. 4: Equilibration time for Model I. (a)  $t_{eq}$  as a function of  $N$  for  $\beta = 3.9$  (circles), 5.8 (pentagons), 11.6 (down-triangles), 12.9 (squares), 14.5 (diamonds), 16.6 (up-triangles); the lines have slopes of 1 (upper) and 2 (lower). (b)  $t_{eq}$  against  $\beta$  for  $N = 490$  (squares), 1000 (triangles), 4000 (circles); the lines have slopes of 3 (left) and 4 (right). Filled symbols correspond to islands and empty ones to pores.

lent agreement with the predicted behavior, to within a trivial prefactor (i. e., slopes agree). Let us remark that the results for island relaxation are given here to allow comparison with the (new) results for pores. We note however a small discrepancy between our numerical results and those of Ref. 7: although the size exponents and activation energies coincide, our equilibration times are found to be lower (by a factor of  $\sim 10$ ) than those reported in Ref. 7.

The corresponding results for Model II are presented in Fig. 5. Note that, also in this case, the theory-simulation agreement is good for both types of structures. Thus, Figs. 4 and 5 confirm our predictions that, on the one hand, the size exponents are universal (1 and 2) and, on the other hand,  $E_R$  and  $E_F$  depend on the specific set of microscopic kinetic barriers.

Finally, in order to test the specific scaling laws, we plot, on a log-log scale,  $(t_{eq}/Nc^5)$  against  $(N/Nc)$  for Model I (Fig. 6) and  $(t_{eq}/Nc^4)$  against  $(N/Nc)$  for Model II (Fig. 7). We have used  $\alpha^I$  and  $\alpha^{II}$  as calculated at the end of Sec. III. According to the analysis presented in Sec. II,  $t_{eq}/Nc^\alpha$  should scale with exponents 1 and 2 for very small and very large values of its argument  $(N/Nc)$ . In Figs. 6 and 7, we have drawn lines with slopes of 1 and

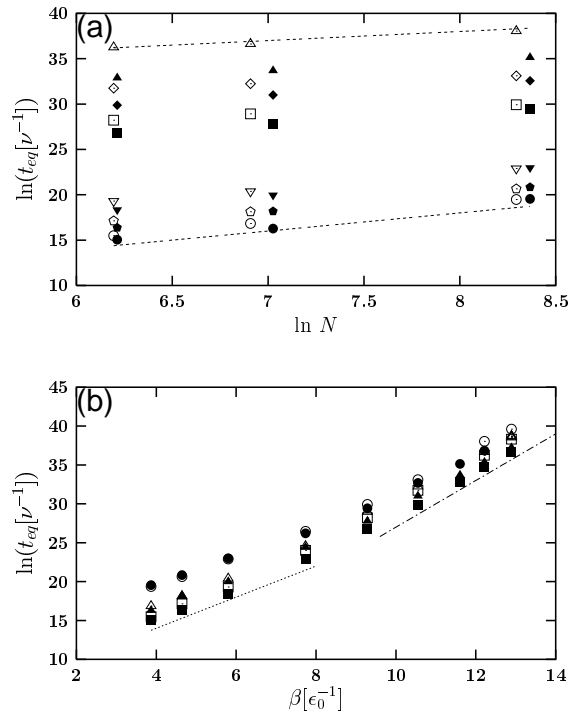


FIG. 5: Equilibration time for Model II. (a)  $t_{eq}$  as a function of  $N$  for  $\beta = 3.9$  (circles), 4.6 (pentagons), 5.8 (down-triangles), 10.6 (squares), 11.6 (diamonds), 12.2 (up-triangles); the lines have slopes of 1 (upper) and 2 (lower). (b)  $t_{eq}$  against  $\beta$  for  $N = 490$  (squares), 1000 (triangles), 4000 (circles); the lines have slopes of 2 (left) and 3 (right). Filled symbols correspond to islands and empty ones to pores.

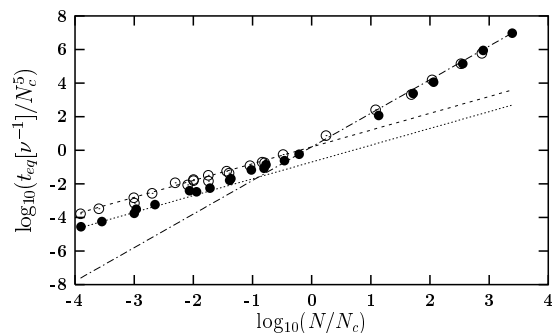


FIG. 6: Model I scaling of  $\log_{10}(t_{eq}/Nc^5)$  against  $\log_{10}(N/Nc)$ , for islands (filled symbols) and pores (empty symbols). The lines have slopes of 1 and 2.

2 to indicate these asymptotic behaviors, which are evidently closely verified. For concreteness, in these plots, we use the same  $Nc = .25 \exp(\beta\epsilon_0)$  as in Ref. 6; the exact value of the geometrical prefactor should not affect the final result in a significant manner.

It is interesting to note that, besides confirming the

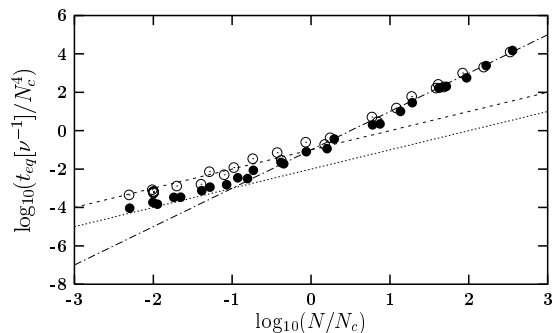


FIG. 7: Model II collapse of data for both islands (filled symbols) and pores (empty symbols). The lines have slopes of 1 and 2

expected asymptotic power laws, in both figures all the points corresponding to islands collapse on one curve, and all the points corresponding to pores collapse on another one (depending via  $\alpha$  on the microscopic details of the model), thus giving additional support to the scaling ansatz. Furthermore, although for each model the island and pore scaling functions are different in the FRM, they become equivalent in the RRM, as required by the perfect pore-island symmetry of relaxation in the latter regime.

## V. CONCLUSIONS

By considering a generic model of adatoms lying on a triangular lattice, we have studied the problem of shape relaxation of islands and pores. The arguments employed in this work allows the main properties of the equilibration time  $t_{eq}$  to be calculated as a function of temperature and size. Because our arguments

are somewhat heuristic, KMC simulations, using two different kinetic models, were also carried out. The numerical results confirm our theoretical predictions. For both islands and pores two qualitatively different modes of relaxation (FRM and RRM) are found, as well as the line  $N_c(T)$  that separates these regimes in the temperature-size plane. It was shown that, although size exponents are universal (1 in FRM, 2 in RRM), the activation energies corresponding to each mode depend on the microscopic details of the kinetic model. Scaling behaviors were found for the equilibration time: the properly scaled  $t_{eq}$  depends also, via  $\alpha$ , on the set of elementary kinetic barriers of the model. Furthermore, for a given model, the specific scaling function for islands is in general different from the one corresponding to pores. While in the FRM both functions scale with the same exponent ( $=1$ ) as a consequence of the detailed-balance condition, in the RRM the two functions collapse because of the perfect island-pore symmetry of HNM theory<sup>5</sup>.

## ACKNOWLEDGMENTS

We are grateful to N. Combe and P. Jensen for interesting discussions. We thank F. Bussi eres, M. de la Chevroti ere, J. Richer, M. Simard and C. Hudon for help with the numerical calculations, and P. Thibault who provided the data needed for Model II. This work was supported by grants from the Natural Sciences and Engineering Research Council (NSERC) of Canada and the ‘‘Fonds Qu eb ecois de la recherche sur la nature et les technologies’’ (FQRNT) of the Province of Qu ebec. We are indebted to the ‘‘R eseau qu eb ecois de calcul de haute performance’’ (RQCHP) for generous allocations of computer resources.

<sup>1</sup> W. K. Burton, N. Cabrera and F. C. Frank, *Phil. Trans. R. Sec. A* **243**, 299 (1951)

<sup>2</sup> M. Lagally, *Phys. Today* **46**(11), 24 (1993).

<sup>3</sup> P. Jensen, *Rev. Mod. Phys.* **71**, 1695 (1999).

<sup>4</sup> Z. Zhang, M. Lagally, *Science* **276**, 377 (1997).

<sup>5</sup> C. Herring, *Phys. Rev.* **82**, 87 (1951); F. A. Nichols, W. W. Mullins, *J. Appl. Phys.* **36** 1826 (1965); W. W. Mullins, *Metall. Mater. Trans. A* **26**, 1917 (1995).

<sup>6</sup> P. Jensen, N. Combe, H. Larralde, J. L. Barrat, C. Misbah, A. Pimpinelli, *Eur. Phys. J. B* **11**, 497 (1999).

<sup>7</sup> N. Combe, H. Larralde, *Phys. Rev. B* **62**, 16074 (2000).

<sup>8</sup> N. Combe, P. Jensen, A. Pimpinelli, *Phys. Rev. Lett.* **85**, 110 (2000)

<sup>9</sup> E. S. Fu, M. D. Johnson, D.-J. Liu, J. D. Weeks, E. D. Williams, *Phys. Rev. Lett.* **77**, 1091 (1996).

<sup>10</sup> C. R. Stoldt, A. M. Cadilhe, C. J. Jenks, J.-M. Wen, J. M. Evans, P. A. Thiel, *Phys. Rev. Lett.* **81**, 2950 (1998).

<sup>11</sup> R. L. Schwoebel, *J. Appl. Phys.* **40**, 614 (1969); R. L.

Schwoebel, E. J. Shipsey, *J. Appl. Phys.* **37**, 3682 (1966); J. Villain, *J. Phys. I France* **1**, 19 (1991).

<sup>12</sup> G. Henkelman, B. P. Uberuaga, H. J onsson, *J. Chem. Phys.* **113** 9901 (2000)

<sup>13</sup> P. Thibault, * tude dynamique et   l’ quilibre de la formation spontan ee de r eseaux d’ lots contraints*, M emoire de ma trise, Universit e de Montr eal (2002).